The following manuscript entitled “Defining the critical material attributes of lactose monohydrate in carrier based dry powder inhaler formulations using artificial neural networks“ has been published in AAPS Pharm Sci Tech, August 2014, Volume 15, Issue 4, pp 1009-1020

DOI: 10.1208/s12249-014-0108-9

Copyedited version can be downloaded at http://link.springer.com/article/10.1208/s12249-014-0108-9

Defining the critical material attributes of lactose monohydrate in carrier based dry powder inhaler formulations using artificial neural networks

Hanne Kinnunen[1], Gerald Hebbink[2], Harry Peters[2], Jagdeep Shur[1] and Robert Price[1*]

[1]Pharmaceutical Surface Science Research Group, Department of Pharmacy and Pharmacology, University of Bath, BA2 7AY, UK.

[2]DFE Pharma, Klever Strasse 187, 47574 Goch, Germany.

***Corresponding author:**
Robert Price PhD,
Telephone: +44 (0) 1225 383644; Fax: +44 (0) 1225 386114
E-mail: r.price@bath.ac.uk

Abstract

The study aimed to establish a function-based relationship between the physical and bulk properties of pre-blended mixtures of fine and coarse lactose grades with the *in vitro* performance of an adhesive active pharmaceutical ingredient (API). Different grades of micronised and milled lactose (Lactohale (LH) LH300, LH230, LH210 and Sorbolac 400) were pre-blended with coarse grades of lactose (LH100, LH206 and Respitose SV010) at concentrations of 2.5, 5, 10 and 20 %w/w. The bulk and rheological properties and particle size distributions were characterised. The pre-blends were formulated with micronised budesonide and *in vitro* performance in a Cyclohaler device tested using a Next Generation Impactor (NGI) at 90 l/min. Correlations between the lactose properties and *in vitro* performance were established using linear regression and artificial neural network (ANN) analyses. The addition of milled and micronised lactose fines with the coarse lactose had a significant influence on physical and rheological properties of the bulk lactose. Formulations of the different pre-blends with budesonide directly influenced *in vitro* performance attributes including fine particle fraction, mass median aerodynamic diameter and pre-separator deposition. While linear regression suggested a number of physical and bulk properties may influence *in vitro* performance, ANN analysis suggested the critical parameters in describing *in vitro* deposition patterns were the relative concentrations of lactose fines %<4.5 µm and %<15 µm. These data suggest that, for an adhesive API, the proportion of fine particles below %<4.5 µm and and %<15 µm could be used as a critical material attributes in rational DPI formulation design.

Keywords: Lactose, dry powder inhaler, quality-by-design, critical material attributes, cohesive-adhesive balance.

Introduction

Carrier based dry powder inhaler (DPI) formulations are a common vehicle for the delivery of highly cohesive drug powders to the lungs, and use the patients' inspiratory effort for fluidising a dose of powder mixture of lactose monohydrate and drug [1]. Ternary components, such as magnesium stearate or fine particle lactose [2], are typically added to the formulation to further optimise and control the detachment and deagglomeration efficiency of the drug particles from the large carrier particles [3].

DPI drug products are an example of a complex dosage form, with many factors that influence drug product functionality and stability [4]. With the introduction of a quality-by-design (QbD) initiative by the US Food and Drug Administration (FDA), pharmaceutical companies have been encouraged to further understand their chemistry, manufacturing and controls (CMC) and their influence on product performance [5]. The current QbD paradigm focuses on the development of product and process design understanding to enable development of drug product that meet the target product profile [6]. In order to achieve this, the QbD approach warrants the development of mechanistic models that correlate critical material attributes (CMAs e.g. raw material physicochemical properties), critical process parameters (CPPs) and product functionality [6]. However, establishing a process and property function relationship for DPI formulation performance has proved to be a challenging task. This is most likely due to the lack of precise control of CPPs and incomplete investigation of CMAs that may directly influence the performance attributes of the product [7].

In the case of DPIs, the excipient plays a critical role in the functionality of the drug product [8]. Indeed, a number of CMAs of lactose monohydrate have been identified that affect DPI drug product quality. For example, surface energy of the lactose measured by inverse gas chromatography [9], specific surface area [10], fine lactose particle content [11,12] and the energy required to fluidise the carrier [13]. These studies suggest, based on relatively small datasets, that a range of parameters adequately characterise the functional behaviour of the lactose and its relationship to drug product quality. However, there has been limited success in developing a mechanistic approach to define the CMAs of lactose monohydrate that influences drug product performance.

Current approaches rely heavily on the use of design of experiments (DoE) and multivariate data analysis (MVA) to understand the relationship between drug and excipient CMAs on drug product performance [14]. These approaches depend on composite experimental design that is applied to define the design space for drug product performance for a range of formulation and process

factors. Response variables are predicted quantitatively from the combination of these factors. Such approaches have been successfully utilised in the development of drug products and have become an integral part of pharmaceutical development risk management. With respect to DPI formulations, these approaches represent a systematic approach to developing theoretical relationships between complex factors and outputs. Podczeck recognised the need for more complex statistical analysis methods for understanding structure-function relationships in DPI formulations [15]. Zeng *et al.* established a two parameter model for the fine particle delivery from DPI formulations based on parameters describing the macroscopic shape of the carrier particles [16]. In both studies, multiple linear regression (MLR) was used for establishing the relationship between lactose properties and DPI formulation performance. The MLR approach is based on the assumption that the underlying relationships are linear and that the input parameters are not co-linear. However, controlling input variables, especially in case of lactose carriers where the main aim during production is the control of the particle size distribution, so that co-linearity is avoided is difficult unless experimental design is applied [17]. These approaches do rely on multiple regression analysis to enable prediction of response variables on the basis of a second-order polynomial equation. Optimisation algorithms are then applied to define the design space. Prediction of pharmaceutical responses based on polynomial relationships is limited and result in poor estimation of drug product design space [18].

In order to overcome the shortcomings of the DoE and MVA approach, a multi-objective simultaneous optimisation approach incorporating artificial neural networks (ANN) are gaining popularity in pharmaceutical drug delivery applications. ANNs are a computational data analysis tool that attempt to incorporate the human brain's capability of learning, adapting and tolerating faulty and noisy data to modern computers' superior ability to perform numerical computation and symbol manipulation [19]. In practice, modelling data using ANNs is based on presenting the data to the network and training the network to recognise the underlying trends in the dataset [19]. Pharmaceutical examples include understanding how flow properties of excipients relate to the micromeritic properties of the materials [20], modelling drug dissolution [21], optimising formulations for controlled release tablets [22] and transdermal drug delivery products [23]. Hitherto, the use of artificial neural network analysis in inhalation research has been limited to modelling *in vivo - in vitro* correlations of inhalation formulations [24] and clinical effects of inhaled bronchodilators with the physiological parameters of individual patients [25].

This study aims to further understand the function-based relationship between particle size, bulk property and powder rheological CMAs of lactose blends, prepared with different coarse carriers and milled and micronised lactose fines, and their influence on key performance attributes of an adhesive, micronised budesonide. Linear regression and artificial neural network (ANN) analysis

was performed in an attempt to determine how these lactose CMAs influence DPI drug product performance.

Materials and methods

Materials

Micronised budesonide was supplied and used as received from Sterling S.r.l (Perugia, Italy). Three different coarse lactose carriers and four different grades of commercially available fine particle lactose were used in the study. Two of the coarse carriers were Lactohale (LH) products, namely LH100 (Sieved coarse grade) and LH206 (Lightly milled coarse grade), and the third coarse carrier was Respitose SV010 (Sieved coarse grade), all samples were kindly donated by DFE Pharma (Borculo, Netherlands). Three of the different fine particle lactose fractions were also Lactohale grades, namely LH300 (micronised fines), LH230 (finer milled fines) and LH210 (coarser milled fines), also from DFE Pharma. The fourth fine particle lactose grade used was Sorbolac 400 from Meggle (Wasserburg am Inn, Germany).

Water used during the studies was Milli-Q reverse osmosis purified (Merck Millipore, Darmstadt, Germany) and methanol and acetonitrile were of HPLC grade and purchased from Sigma (Gillingham, UK).

Preparation of lactose pre-blends

Carrier lactose pre-blends were prepared by adding different fractions of the fine lactose samples to the coarse carriers at 2.5, 5, 10 and 20 %w/w concentrations, as summarised in Table I. All lactose pre-blends were produced in 100g batches. The fine lactose grades were sandwiched between the coarse carrier in either two (2.5% blends) or three layers (5, 10 and 20% blends) in a stainless steel cylindrical vessel with an internal diameter of 100 mm and a height of 150 mm. The headspace in the vessel was approximately two thirds of the volume of the container, depending on the fines content of the pre-blend. The mixtures were blended with a Turbula mixer (Glen Creston, Middlesex, UK) at 46 rpm for 60 minutes. All pre-blends were stored at 44±1% relative humidity (RH) and 20±2°C for at least 7 days before any further work was carried out.

Particle size measurements

The particle sizing of the raw materials and pre-blends was conducted using a HELOS laser diffraction unit in conjunction with Windox 5 software, both from Sympatec GmbH (Clausthal-Zellerfield, Germany). The high resolution Fraunhofer model (HRLD) provided by the Windox

software was used for calculating the particle size distributions of all the materials from the raw scattering data.

The particle size of lactose raw materials and pre-blends were measured using a validated methodology, utilising the R4 lens and the RODOS dry powder disperser in conjunction with the Vibri dry powder feeder. The feed rate was adjusted such that an optical concentration of between 0.5% and 5% was achieved. No data was recorded until a threshold value of 0.5% for optical concentration was exceeded. A dispersion pressure of 2 bar was used for measuring the lactose samples. The background scattering was recorded for ten seconds with the vacuum on and five repeated measurements of two seconds duration were recorded for the lactose samples.

The PSD of micronised budesonide was characterised using a R3 lens and a Cuvette wet dispersion system. An aliquot of the material was dispersed in cyclohexane that contained 0.1% lecithin to aid the dispersion. The stirring speed was set to 1500 rpm. Prior to PSD measurements, the background scattering was recorded for a period of 10 seconds. To achieve a measure of the primary particle size, the suspension was ultrasonicated at 50% intensity of the maximum with the internal probe of the disperser system for one minute. After ultrasonication, the final optical concentration was between 3 and 10%. Five repeated measurements of five seconds were recorded for the drug.

Cohesive-adhesive balance (CAB) measurements of budesonide

A random selection of particles from the micronised batch of budesonide were attached onto standard V-shaped tipless cantilevers with pre-defined spring constants (DNP-020, DI, CA, USA) using an epoxy resin glue (Araldite, Cambridge, UK), using a previously described method **[26]**. A minimum of five probes were prepared and all colloid probes were examined with an optical microscope (magnification 50x) to ensure the integrity of the attached particle, before and after colloid probe force measurements.

The crystal face of a primary crystallised sample of budesonide was used for atomic force microscopy-cohesive adhesive balance (AFM-CAB) measurements as described previously **[26]**. To measure the force of adhesion (drug-excipient) a smooth surface of lactose was also crystallised, as described elsewhere [26]. The surface roughness as measured by the R_a and R_q of the surfaces of crystal particles of budesonide and lactose were <1 nm and therefore suitable for CAB measurements.

Substrates were loaded on to the AFM scanner stage, which was enclosed in a custom-built environmental chamber, in which the ambient conditions were maintained at a constant

temperature of 25 ± 1.5°C and relative humidity of 35 ± 3%. The interactive forces of the colloid probes with the lactose and budesonide substrates were measured by recording the deflection of the AFM cantilever as a function of the substrate displacement (z) by applying Hooke's Law (F = -kz). Individual force curves (n = 1024) were collected over a 10 µm x 10 µm area using the force volume mode at a scan rate of 4 Hz and a compressive load of 40 nN. Parameters were kept constant over the study. Quantification of the nominal spring constant of each cantilever was performed using a dynamic method of thermal noise analysis [27].

With the vast array of data generated during force volume measurements, custom-built software was used to extract data. These collected force data were analysed to ensure normal distribution, indicating uniform contact between the drug probe and excipient substrate. Arithmetic mean and standard deviation were obtained from force data and used to produce the CAB plot.

Powder bulk properties and flow and fluidisation characteristics

Bulk and tapped densities (ρ_B and ρ_T, respectively) were measured using the FT4 powder rheometer (Freeman Technology, Tewkesbury, UK). For bulk density measurements, a 25 mm diameter, 20 ml volume split measurement vessel was placed on the measurement table of the instrument and the weight of the vessel tared. The vessel was then filled with the powder under investigation. A conditioning cycle was run to remove the influence of the filling procedure on powder packing. For measuring the bulk density, the measurement vessel was split and the split powder mass recorded. For tapped density measurements, the vessel was placed on a jolting volumeter (J. Engelsmann, Ludwigshafen, Germany) and 250 taps were applied. The vessel was then transferred back to the FT4 and the split powder mass recorded. All the measurements were performed in triplicate. The Hausner ratio (HR) that is a measure of the flow properties of powders with a value <1.25 indicating a free flowing powder and >1.25 indicating a poor flowing powder [28], was calculated according to Equation 1:

$$HR = \frac{\rho_T}{\rho_B} \quad \textbf{(1)}$$

The FT4 powder rheometer can be used for characterising flow properties of powders under different conditions to simulate the behaviour of powders while they are exposed to different environments during processing and usage. The normalised basic flow energy (BFE_{Norm}) is a general descriptor of powder flow properties and characterises the resistance of one gram of a chosen powder to flow under a constant speed with cohesive powders exhibiting low BFE_{Norm} [29]. The flow rate index (FRI) measurement on the other hand is a dimensionless parameter describing how different powders react to changes in the rate at which an impeller blade is traversed in a helical path. It has been shown that more cohesive powders appear to be more sensitive to such

changes and therefore have higher FRI [29]. Specific energy (SE) is a parameter based on the force and torque measured in the rheometer during upward blade motion. The value of SE describes the flow properties of the powders in a stress free state at near zero consolidation due to the lack of a downward loading force by the blade [29]. The BFE_{Norm}, FRI and SE were measured during the same test procedure using a purpose-built measurement program. For these measurements, the powder was loaded in the 25mm bore diameter, 20 ml volume split vessel. At first, a downward conditioning cycle was run at a tip speed of -40 mm/s and a helical angle of 5° to remove the packing history of the powder. This was followed by an upward conditioning cycle at a tip speed of 40 mm/s and a helical angle of 5°. After conditioning, the measurement cell was split and the split mass recorded. Consecutive cycles of conditioning and BFE measurements were repeated seven times at a tip speed of -100 mm/s and helical angle of -5° to assess the stability of the powder under agitation. If the powder was observed to be stable, the BFE measured during the 7^{th} measurement cycle was divided by the split mass to calculate the BFE_{Norm}. SE was defined as the energy required to lift the blade out of the powder bed and was also measured during the 7^{th} measurement cycle. To measure the FRI, four additional measurement cycles at tip speeds -100, -70, -40 and -10 mm/s were run with an unaltered conditioning cycle between each of them. The FRI was calculated as the ratio of the flow energy measured at a tip speed of -10mm/s over the flow energy measured at a tip speed of -100 mm/s.

The normalised fluidisation energy (FE_{Norm}) is defined as the energy required to keep the impeller blade moving through one gram of fluidised powder bed at a constant speed. The lower the value, the more easily the powder can be fluidised. Dynamic flow index (DFI) describes the reactivity of the powder to an air flow through the powder bed. The higher the value of DFI, the more the powder structure is affected by the fluidising gas flowing through the powder bulk. The FE_{Norm} and DFI were measured during the same measurement program. Powders were loaded into a 25mm bore diameter, 20ml volume split vessel. An initial conditioning cycle was repeated 8 times at a tip speed of -60 mm/s downward and 60 mm/s upward and helical angles of 5° and -5°, respectively, to remove the packing history of the powder. After the initial conditioning, the measurement cell was split. A cycle of conditioning and measuring was then repeated at different air velocities, controlled by an aeration control unit (ACU) of an FT4. The air velocity was adjusted such that, during the conditioning cycle, the air velocity was equal to the air velocity of the following measurement. The measurement cycles at the different air velocities were performed at a tip speed of -100 mm/s and a helical angle of -5° followed by an upward motion at a tip speed of 60mm/s and a helical angle of 10°. The FE_{Norm} was calculated by dividing the fluidisation energy at the point where the powder became fully fluidised (no further decrease in flow energy upon increasing fluidising gas velocity) with the split mass of the powder bed. The DFI was calculated as the ratio between the flow energy at fluidising gas velocity of 0 mm/s by the flow energy at the minimum fluidisation velocity.

Preparation and in vitro testing of budesonide DPI formulations

Carrier based DPI formulations of micronised budesonide at 0.8 %w/w concentration with the different lactose pre-blends were prepared using a Turbula mixer at 46 rpm in 40 g quantities in the same blending vessel that was used for the preparation of the lactose pre-blends. Briefly, lactose blends were all passed through an 850µm aperture sieve to break any large agglomerates which may have formed during storage. A quarter of the mass of the lactose required was transferred to the blending vessel and the drug was sandwiched with another quarter the lactose pre-blend. This was blended for 10 minutes. The remaining half of the lactose was then added and blended for a further 45 minutes. After blending, formulations were passed through a 250 µm sieve and stored at 20 ± 2°C and 44% RH for at least a week before the content uniformity of the blends was assayed.

Content uniformity was analysed by taking ten random 12.5mg aliquots from each formulation. The drug content was assayed using high performance liquid chromatography (HPLC). The acceptance criteria for blend content uniformity were set according to USP<905> [30]. Formulations were subsequently hand-filled into size 3 Quali-V hydroxypropylmethylcellulose (HPMC) capsules (Qualicaps, Madrid, Spain) with a fill weight of 12.5 mg.

In vitro performance of the formulations was assessed using a Next Generation Impactor (NGI) equipped with a pre-separator (Copley Scientific, Nottingham, UK). A Cyclohaler DPI device (Teva Pharmaceuticals, The Netherlands) was used at a flow rate of 90 litres per minute with 4L of air being drawn through the device. All impactor stage plates and the pre-separator were pre-coated with silicone oil and 15 ml of mobile phase was placed in the collection cup of the pre-separator before two capsules were aerosolised into the impactor. The drug deposited in the different stages of the impactor was assessed by dissolving the particles collected in mobile phase and analysing the drug content by HPLC. The fine particle fraction of emitted dose (FPF_{ED}) and mean mass aerodynamic diameter (MMAD) were determined by interpolation based on the mass of particles finer than 5 µm collected in the impactor, determined by regression analysis. The proportion of drug deposited in the pre-separator (PS of RD) was used as an indicator of the efficiency of drug detachment from the large lactose crystals [31].

High performance liquid chromatography (HPLC) drug analysis

The samples were dissolved in a mobile phase that consisted of 20% water, 35% acetonitrile and 45% methanol. The mobile phase was pumped through the HPLC system at a flow rate of 1.5 ml/min using a PU-980 pump (Jasco, Tokyo, Japan). 100 µl of the samples were injected into the system using an AS-950 autosampler (Jasco, Tokyo, Japan). The 250 mm long Hypersil-ODS column with an inner diameter of 4.6mm and packing material particle size of 5 µm (Thermo

Scientific, Loughborough, UK) was held at 40°C using a CO-965 column oven (Jasco, Tokyo, Japan). The eluted drug was detected using a UV-975 detector (Jasco, Tokyo, Japan) at a wavelength of 244 nm for budesonide. The retention time for budesonide was 3.75 min.

Statistical analysis

Linear correlations between the physical properties of the lactose carriers and the DPI performance of the formulations were established using Minitab v.15 statistical analysis package (Minitab Ltd, Coventry, UK). The strength of the linear correlation between the lactose properties and the DPI performance attributes was evaluated by the value of r ($-1<r<1$), with perfect correlation producing a value of 1 and the sign denoting the direction of the correlation.

Artificial neural network analysis of the dataset

The hierarchy, design and theoretical basis of ANNs can be found elsewhere [32]. The general structure of ANN has one input layer, many hidden layers and one output layer. Each layer incorporates many units corresponding to “neurons”, which are fully interconnected with links corresponding to synapses [32]. The strength of connections between two units are called “weights”. In each hidden layer and output layer the processing unit sums the input from the previous layer and then applies a sigmoidal function to compute its output to the following layer according to the following equations:

$$\gamma_q = \sum w_{pq} x_p \quad (2)$$

$$f(\gamma_q) = 1/\{1 + \exp(-\alpha\gamma_q)\} \quad (3)$$

where w_{pq} is the weight of the connection between unit q in the current layer to unit p in the previous layer, and x_p is the output value from the previous layer [33]. The $f(\gamma_q)$ is conducted to the following layer as an output value. Alpha is a parameter relating to the shape of the sigmoidal function, which is strengthened with an increase in alpha [18]. ANN learns an approximate non-linear relationship by a procedure called “training”, which involves varying weight values. Training is defined as a search process for the optimised set of weight values, which can minimise the squared error between the estimation and experimental data of units in the output layer [18]. Training is an iterative process that may lead to under and over-estimation of the predicted output. This however, is avoided through the application of a backpropagation algorithm in combination with either the backsweep or recursive algorithms. The backpropagation algorithm consists of a

forward propagation through a neural network, a backward propagation, and a weight update for each training step [33]. This processing helps to reduce the number of iterations and improves prediction from the neural design. Optimisation and validity of the study is not necessarily determined by the number of samples, but by the plurality of the study design that incorporates many units in each layer of the neural network.

ANN analysis of data was performed using Alyuda Neurointelligence software (Alyuda Neurointelligence, California, USA). The input data were pre-processed so that the range of input values were within the range of [-1…1] and output values within the range of [0…1]. The dataset was partitioned to training, test and validation sets, with 27 records (70%) being used for the training set and 6 (15%) for both the validation and test sets. A batch back-propagation training algorithm was used for the network training. The network architecture was selected manually as 12-4-1 for fine particle fraction of the emitted dose and 12-5-1 for mean mass aerodynamic diameter and pre-separator deposition. The logistic transfer function **[32]** and sum of squares error function **[34]** were used for determining the firing intensity of a neuron and the error between the actual and predicted output, respectively. For all the networks, a momentum of 0.9 was used. The learning rate was set to 0.1 for the ANN modelling of the fine particle fraction of the emitted dose and pre-separator deposition, and 0.25 for the ANN network modelling of the mean mass aerodynamic diameter. In all cases, network training was stopped by error change when the mean square error of the network or the dataset error over 10 training cycles changed by less than 0.0000001.

Results and Discussion

Physicochemical characterisation of the raw materials

The particle size distribution (PSD) of the micronised budesonide is shown in Figure 1. The d_{10}, d_{50} and d_{90} of the budesonide batch were 0.80, 2.08 and 4.4µm, respectively. The mean force of cohesion (drug probe interaction with drug crystal) of five probes of the micronised budesonide were plotted against the corresponding mean force of adhesion (drug probe interaction with lactose crystal) to form the CAB plot, as shown by Figure 2. Linear regression analysis through the origin of the CAB data showed a linear fit with a regression coefficient of 99.8%. The gradient of each plot was equated to determine the CAB ratio of the micronised budesonide. The CAB value of the micronised budesonide 0.62 ± 0.02 was similar to previously reported CAB measurements of commercially supplied micronised budesonide with lactose monohydrate [35,36]. These data suggest that for an equivalent force of cohesion the adhesion of the micronised budesonide to lactose is approximately 1.61 times greater than its drug-drug interaction and is therefore a highly suitable candidate molecule for investigating the role of fines for an adhesive drug.

The particle size distributions of the coarse lactose (LH100, LH206 and SV010), micronised lactose fines (LH300) and milled fine lactose grades (LH230, LH210 and Sorbolac 400) are shown in Figure 3 and their characteristic properties summarised in Table II. The rank order of the level of intrinsic lactose fines (%≤4.5µm) of the coarse carriers are LH206 > SV010 > LH100. The corresponding order for the fine lactose fractions is LH300 > LH230 > LH210 ~ Sorbolac 400. Despite LH210 and Sorbolac 400 having similar proportions of %<4.5 µm, in terms of d_{10}, d_{50} and d_{90} and particle size distributions (Figure 3) LH230 and Sorbolac 400 are similar to each other.

Physical and bulk powder characterisation of lactose pre-blends

The fine lactose particle content of the pre-blends from particle size measurements are summarised in Table III. These data indicate that the proportion of lactose fines below 4.5 µm ranged between 1.3% and 23% and the proportion of particles finer than 15 µm and 30 µm ranged from 2.5 to 40% and 3.8 to 43%, respectively. These differences in the fines content within the pre-blends were also reflected by variability in the d_{10} values of the carrier blends, which ranged between 1.7 and 50 µm.

The corresponding bulk and tapped densities and powder flow and fluidisation properties of the carrier pre-blends are summarised in Table IV. The Hausner ratio for the pre-blends varied between 1.14 and 1.54. Carriers that exhibited the lowest Hausner ratios corresponded to the pre-

blends that contained no added lactose fines. The addition of lactose fines significantly increased the Hausner ratio and thereby reduced the flowability of the pre-blends.

These findings were confirmed by powder rheological measurements of the lactose pre-blends, tabulated in Table IV. A range of rheological properties were analysed including the basic flow energy (BFE_{norm}) and fluidisation energy (FE_{norm}), which were both normalised to the powder mass tested, the dynamic flow index (DFI), flow rate index (FRI) and specific energy (SE). In general, as powders became more cohesive the FE_{Norm} and FRI increase while the BFE_{norm} and DFI values decrease [29]. Therefore, the flow and fluidisation parameters measured for the carriers suggested that increasing the amount of lactose fines reduced the flowability and increased the energy required to fluidise the pre-blends. Unlike the Hausner ratio measurements, which were relatively insensitive to the type of fines (micronised vs. milled) present in the pre-blend, powder rheological data suggested that at high concentration micronised lactose fines had the most significant effect on reducing flow and increasing the cohesive properties of the pre-blends. In summary, the parameters describing the flow and fluidisation properties of the lactose pre-blends indicated that increasing fines content increased the cohesive strength of the lactose pre-blend. This is in an agreement with reported studies of Shur *et al.*, who suggested that upon addition of lactose fines an increase in the cohesive strength is observed, which in turn may lead to greater deagglomeration efficiency of the micronised drug and thereby improving performance [37].

In vitro aerodynamic particle size distribution (APSD) testing of budesonide DPI formulations

The results of the *in vitro* aerodynamic particle size distribution (APSD) measurements of the budesonide formulations prepared with all 39 different pre-blends, aerosolised from a Cyclohaler at 90 l/min, are summarised in Table V. The results were recorded as fine particle fraction of emitted dose (FPF_{ED}), mean mass aerodynamic diameter (MMAD) and the proportion of drug recovered from the pre-separator (PS of RD).

The fine particle delivery (FPF_{ED}) of budesonide (Table V) was significantly affected by the type and level of lactose fines added to the three different coarse grades of lactose (LH100, LH206 and SV010, see Table I), and ranged between 20.8% and 46.9%. For the capsule-based Cyclohaler device, the addition of the micronised LH300 fines to the coarse carriers had the most significant influence on increasing the fine particle fraction, and concomitantly reduced the amount of drug retained on the coarse lactose recovered from the pre-separator. However, despite increasing the cohesive strength of the lactose carrier pre-blends, the addition of the milled fines (LH230, LH210 and Sorbolac 400) did not lead to as significant an improvement in the DPI performance as the addition of micronised LH300 lactose fines. These data suggest that the increasing the cohesive

strength of the formulation may not be the dominant attribute in improving performance upon the addition of Geldart group C fines [38].

For all formulations, the MMAD of the drug increased with increasing levels of milled and micronised fines, ranging from 2.58 µm to 3.51 µm. These data suggest that agglomeration and co-deposition of the API with lactose fines on the impactor stages may have occurred.

Linear correlations between the physical properties of the carrier and the *in vitro* performance of the formulations

Linear correlations have been previously observed between different parameters relating to lactose properties and DPI performance on relatively small datasets [9,11,39]. Thus, the initial approach utilised in understanding the critical attributes of lactose fines and how they may influence the bulk powder properties and govern deagglomeration and drug detachment efficiency of DPI formulations, was to conduct statistical analysis for linear correlations for the current dataset.

The correlation coefficients (*r*) from these analyses are summarised in Table VI and shown in Figure 4. These data (Table VI and Figure 4A) indicate that in predicting the fine particle fraction of emitted dose (FPF_{ED}), the percentage of fine particle lactose %≤4.5 µm in the carrier produced the best linear correlation with an $r = 0.861$. These data are in good agreement with studies published by various other researchers where the proportion of lactose fines was shown to correlate directly with DPI performance [11,12,14]. It is also notable that in the current study the *r* value between different particle size parameters decreased from 0.861 to 0.740 and 0.638 when the fines fraction percentages were measured as %≤4.5 µm, %≤15 µm and %≤30 µm, respectively. These data are also in an agreement with a previous study where the finer fractions of lactose were seen to produce a better correlation with DPI performance [40].

One of the theories for explaining the improvement in DPI performance with fines is that the fluidisation properties of the bulk powder change due to an increase in cohesive strength upon the addition of Geldart type C [38] fine powders [37]. To test this theory, the correlation coefficients for linear correlations between the cohesive properties of the carriers (Table IV) and FPF_{ED} are shown in Table VI. The FPF_{ED} had positive correlations of 0.748, 0.649 and 0.578 against FE_{Norm}, Hausner ratio and FRI, respectively. The relationship between the BFE_{Norm} and FPF_{ED} was characterised by a negative correlation of -0.664. These results suggest that, indeed, the more cohesive the carrier blend, the higher the DPI formulation performance. However, because the *r* values are relatively low, the linear models based on flow and fluidisation properties of the carrier appeared not to be able to differentiate variations in the different grades of lactose fines with the FPF_{ED}.

Figure 4A and Table VI indicate that linear correlation analysis of the MMAD as a function of the carrier properties produced the highest degree of correlation for the proportion of fines %≤15 µm and %≤30 µm with an r = 0.907 and r = 0.924, respectively. These data further indicate the complex nature of these formulations, where the interaction of the drug with coarser fines leads to a significant increase in aerodynamic diameter of the aerosolised drug, while having a minimal influence on increasing fine particle delivery. It has been previously suggested that these fines may be of sufficient size to act as secondary carriers [40].

The strongest correlation between the physical properties of the lactose blends and the pre-separator deposition was with FE_{Norm} with an r = -0.891, together with %<15 µm and %<4.5 µm with a coefficient of determination of -0.885 and 0.882, respectively (Figure 4C and Table VI). These data indicate that the fluidisation properties of the lactose carrier alongside the fine particle content may be important in determining the extent of drug detachment from the surface of the large carrier crystals.

It is noteworthy, as highlighted in Figure 4, that linear correlation analysis of the comparatively large dataset appeared to produce relatively high correlation coefficients for all the different parameters utilised for describing the properties of the lactose pre-blends. It is, therefore, not surprising that when smaller datasets are investigated, good linear correlations are frequently reported between carrier properties and DPI performance.

Artificial neural network analysis of the datasets

In the current study, the ANN was used as a tool for predictively understanding the complex behaviour of how lactose fines govern DPI performance of an adhesive drug in a Cyclohaler. By inspecting the relative importance of the different input parameters of the lactose powders in the trained networks, the importance of each of the parameters could be measured against the different performance indicating attributes associated with DPI performance. These data are summarised in Table VII.

The relative importance of the different input parameters in the network modelling FPF_{ED}, listed in Table VII, is shown in Figure 5A. The proportion of fines below %<4.5 µm was the most important parameter, with over 57% of the connection weights derived from this parameter. This is in an agreement with the outcome of linear statistical model based on the highest r values. The rheological FRI measurement was also shown to correlate with the FPF_{ED}, but to a considerably lower degree of importance.

In modelling the MMAD, the proportion of fines %<15 µm was by far the most important parameter with 76% of the connection weights in the ANN being derived from the single parameter. These data are shown in Table VII and illustrated in Figure 5B. This indicates, that although the proportion of fines %<4.5 µm was the most important parameter in determining the DPI performance as defined by FPF_{ED}, coarser fines may play a role in determining the extent of deagglomeration of the drug.

As shown in Table VII and Figure 5C, the proportion of lactose fine particles %<4.5 µm was the most important parameter in relation to drug deposition in the pre-separator with a 46% connection weight. These data suggested that an increased percentage in the proportion of fine particle lactose particles %<4.5 µm with respect to the coarser size fractions of the fines led to the decrease in the drug deposition in the pre-separator. This is supported by the fact that the second most important parameter was the 10^{th} percentile of the particle size distribution (d_{10}).

From the ANN data (Figure 5 and Table VII), a number of different physical and bulk powder parameters characterised for the lactose pre-blends appeared to have a relatively small influence on DPI performance attributes. These were mainly the flow related measurements of specific energy, tapped density and Hausner ratio.

The results also suggested that there might be a direct correlation between efficiency of drug detachment from the carrier and fine particle fraction delivery. The deagglomeration efficiency of the drug from the carrier, as measured by the proportion of drug collected in the pre-separator as a function of the recovered dose, was mainly affected by the proportion of the finer (%<4.5 µm) lactose fines, as was also the FPF_{ED}. These findings suggest that a significant reduction in pre-separator deposition is achieved with greater concentrations of finer (%<4.5 µm) lactose. An increasing concentration of %<15 µm lactose fines with respect to the concentration of fines (%<4.5 µm) may lead to a greater drug retention of the drug on the lactose at the pre-separator, which supports the theory that the coarser fraction of milled lactose fines may be acting as secondary carriers [40].

The addition of these coarser fines was also shown to affect the aerodynamic particle size distribution of the API, as measured by the MMAD. For the ANN model, the proportion of fines %<15 µm appeared to influence the MMAD of the budesonide. These models suggest that an increase in the relative amount of the lactose fines between 4.5 µm and 15 µm and possibly up to 30µm leads to the shift in the aerodynamic diameter of the measurements of the API, with greater deposition of the drug on the upper stage of the impactor.

These data suggest that for a population of data, the ANN methodology may help in identifying key CMAs of lactose that affect drug product quality. In the context of QbD, this may allow greater understanding of material properties that may affect drug product behaviour and can therefore be utilised to control and continually improve the drug product.

Conclusions

The performance of DPI formulations appears to be governed by a multitude of excipient properties that often cannot be changed in a controlled manner or independently from one another. In this study, ANN analysis of the structure-function data was used together with linear regression to obtain a more complete understanding of the cause and effect relationship of the influence of fine lactose on the DPI performance of an adhesive drug in a capsule-based inhaler device. Linear regression of the datasets suggested a number of physical and bulk related properties might influence the key *in vitro* performance parameters. ANN analysis suggested that the only critical parameters required in describing the *in vitro* deposition patterns were the relative measurements of the concentration of lactose fines %<4.5 µm and %<15 µm. For the ANN model, the deagglomeration efficiency as measured by fine particle delivery performance was pre-dominantly governed by the proportion of fine lactose particles %<4.5 µm and the proportion of fine lactose particles %<15 µm appeared to govern the increase in the MMAD of the drug. ANN analysis suggested that the most dominant property in decreasing the amount of drug retained in the pre-separator was the percentage of fines below %<4.5 µm.

Acknowledgements

DFE Pharma for funding the study and Prof Eddie French for providing feedback on the manuscript.

References

1. Chan H-K. Dry powder aerosol delivery systems: current and future research directions. J Aerosol Med. 2006;19:21–7.

2. Guchardi R, Frei M, John E, Kaerger JS. Influence of fine lactose and magnesium stearate on low dose dry powder inhaler formulations. Int J Pharm. 2008 Feb 4;348:10–7.

3. Louey MD, Stewart PJ. Particle interactions involved in aerosol dispersion of ternary interactive mixtures. Pharm. Res. 2002 Oct;19:1524–31.

4. Lee SL, Adams WP, Li BV, Conner DP, Chowdhury BA, Yu LX. In vitro considerations to support bioequivalence of locally acting drugs in dry powder inhalers for lung diseases. AAPS J. 2009 Sep;11:414–23.

5. Yu LX. Pharmaceutical quality by design: product and process development, understanding, and control. Pharm. Res. 2008 Apr;25:781–91.

6. Lionberger RA, Lee SL, Lee LM, Raw A, Lawrence XY. Quality by design: concepts for ANDAs. AAPS J. 2008;10:268–76.

7. de Boer AH, Chan HK, Price R. A critical view on lactose-based drug formulation and device studies for dry powder inhalation: which are relevant and what interactions to expect? Adv. Drug Deliv. Rev. 2012 Mar 15;64:257–74.

8. Edge S, Mueller S, Price R, Shur J. Factors affecting defining the quality and functionality of excipients used in the manufacture of dry powder inhaler products. Drug Dev Ind Pharm. 2008 Sep;34:966–73.

9. Traini D, Young PM, Thielmann F, Acharya M. The influence of lactose pseudopolymorphic form on salbutamol sulfate-lactose interactions in DPI formulations. Drug Dev Ind Pharm. 2008 Sep;34:992–1001.

10. Jones MD, Harris H, Hooton JC, Shur J, King GS, Mathoulin CA, et al. An investigation into the relationship between carrier-based dry powder inhalation performance and formulation cohesive-adhesive force balances. Eur J Pharm Biopharm. 2008 Jun;69:496–507.

11. Louey MD, Razia S, Stewart PJ. Influence of physico-chemical carrier properties on the in vitro aerosol deposition from interactive mixtures. Int J Pharm. 2003 Feb 18;252:87–98.

12. Islam N, Stewart P, Larson I, Hartley P. Lactose surface modification by decantation: are drug-fine lactose ratios the key to better dispersion of salmeterol xinafoate from lactose-interactive mixtures? Pharm. Res. 2004 Mar;21:492–9.

13. Pitchayajittipong C, Price R, Shur J, Kaerger JS, Edge S. Characterisation and functionality of inhalation anhydrous lactose. Int J Pharm. 2010 May 10;390:134–41.

14. Guenette E, Barrett A, Kraus D, Brody R, Harding L, Magee G. Understanding the effect of lactose particle size on the properties of DPI formulations using experimental design. Int J Pharm. 2009 Oct 1;380:80–8.

15. Podczeck F. The relationship between physical properties of lactose monohydrate and the aerodynamic behaviour of adhered drug particles. Int J Pharm. 1998;160:119–30.

16. Zeng XM, Martin AP, Marriott C, Pritchard J. The influence of carrier morphology on drug

delivery by dry powder inhalers. Int J Pharm. 2000 Apr 25;200:93–106.

17. Rajalahti T, Kvalheim OM. Multivariate data analysis in pharmaceutics: a tutorial review. Int J Pharm. 2011 Sep 30;417:280–90.

18. Takayama K, Fujikawa M, Nagai T. Artificial neural network as a novel method to optimize pharmaceutical formulations. Pharm. Res. Springer; 1999;16:1–6.

19. Jain AK, Mao J, Mohiuddin KM. Artificial neural networks: A tutorial. Computer. 1996;29:31–44.

20. Kachrimanis K, Karamyan V, Malamataris S. Artificial neural networks (ANNs) and modeling of powder flow. Int J Pharm. 2003 Jan 2;250:13–23.

21. Mendyk A, Jachowicz R. Neural network as a decision support system in the development of pharmaceutical formulation—focus on solid dispersions. Expert Systems with Applications. 2005.

22. Barmpalexis P, Kachrimanis K, Georgarakis E. Solid dispersions in the development of a nimodipine floating tablet formulation and optimization by artificial neural networks and genetic programming. Eur J Pharm Biopharm. 2011 Jan;77:122–31.

23. Takayama K, Takahara J, Fujikawa M, Ichikawa H, Nagai T. Formula optimization based on artificial neural networks in transdermal drug delivery. J Control Release. 1999 Nov 1;62:161–70.

24. de Matas M, Shao Q, Richardson CH, Chrystyn H. Evaluation of in vitro in vivo correlations for dry powder inhaler delivery using artificial neural networks. Eur J Pharm Sci. 2008 Jan;33:80–90.

25. de Matas M, Shao Q, Biddiscombe MF, Meah S, Chrystyn H, Usmani OS. Predicting the clinical effect of a short acting bronchodilator in individual patients using artificial neural networks. Eur J Pharm Sci. 2010 Dec 23;41:707–15.

26. Begat P, Morton DAV, Staniforth JN, Price R. The cohesive-adhesive balances in dry powder inhaler formulations I: Direct quantification by atomic force microscopy. Pharm. Res. 2004 Sep;21:1591–7.

27. Kubavat HA, Shur J, Ruecroft G, Hipkiss D, Price R. Investigation into the influence of primary crystallization conditions on the mechanical properties and secondary processing behaviour of fluticasone propionate for carrier based dry powder inhaler formulations. Pharm. Res. 2012 Apr;29:994–1006.

28. Shah RB, Tawakkul MA, Khan MA. Comparative evaluation of flow for pharmaceutical powders and granules. AAPS PharmSciTech. 2008;9:250–8.

29. Freeman R. Measuring the flow properties of consolidated, conditioned and aerated powders—a comparative study using a powder rheometer and a rotational shear cell. Powder Technology. Elsevier; 2007;174:25–33.

30. USP<905> Uniformity of Dosage Units. United States Pharmacopoeia. usp.org; 2011. pp. 1–3.

31. Dickhoff BHJ, Ellison MJH, de Boer AH, Frijlink HW. The effect of budesonide particle mass on drug particle detachment from carrier crystals in adhesive mixtures during inhalation. Eur J Pharm Biopharm. 2002 Sep;54:245–8.

32. Benitez JM, Castro JL, Requena I. Are artificial neural networks black boxes? IEEE Trans Neural Netw. 1997;8:1156–64.

33. Piche SW. Steepest descent algorithms for neural network controllers and filters. IEEE Trans Neural Netw. 1994;5:198–212.

34. Aitkin M, Foxall R. Statistical modelling of artificial neural networks using the multi-layer perceptron. Statistics and Computing. 2003;13:227-239.

35. Hooton JC, Jones MD, Harris H, Shur J, Price R. The influence of crystal habit on the prediction of dry powder inhalation formulation performance using the cohesive-adhesive force balance approach. Drug Dev Ind Pharm. 2008 Sep;34:974–83.

36. Kubavat HA, Shur J, Ruecroft G, Hipkiss D, Price R. Influence of primary crystallisation conditions on the mechanical and interfacial properties of micronised budesonide for dry powder inhalation. Int J Pharm. 2012 Jul 1;430:26–33.

37. Shur J, Harris H, Jones MD, Kaerger JS, Price R. The role of fines in the modification of the fluidization and dispersion mechanism within dry powder inhaler formulations. Pharm. Res. 2008 Jul;25:1631–40.

38. Geldart D. Types of gas fluidization. Powder Technology. 1973;7:285–92.

39. Islam N, Stewart P, Larson I, Hartley P. Lactose surface modification by decantation: are drug-fine lactose ratios the key to better dispersion of salmeterol xinafoate from lactose-interactive mixtures? Pharm. Res. 2004.

40. Handoko A, Ian L, Peter SJ. Influence of the polydispersity of the added fine lactose on the dispersion of salmeterol xinafoate from mixtures for inhalation. Eur J Pharm Sci. 2009 Feb 15;36:265–74.

Table I Summary of the coarse and fine lactose components used for preparing the carrier pre-blends for the current study and the process history and the weight-to-weight % (wt-%) concentrations of the fines present in the different pre-blends

Carrier ID	Coarse fraction	Type of Fines	Fines	Wt-% fines
1	LH100	-	-	0
2	LH100	Micronised	LH300	2.5
3	LH100	Micronised	LH300	5
4	LH100	Micronised	LH300	10
5	LH100	Micronised	LH300	20
6	LH100	Milled	LH230	2.5
7	LH100	Milled	LH230	5
8	LH100	Milled	LH230	10
9	LH100	Milled	LH230	20
10	LH100	Milled	LH210	2.5
11	LH100	Milled	LH210	5
12	LH100	Milled	LH210	10
13	LH100	Milled	LH210	20
14	LH100	Milled	Sorbolac 400	2.5
15	LH100	Milled	Sorbolac 400	5
16	LH100	Milled	Sorbolac 400	10
17	LH100	Milled	Sorbolac 400	20
18	LH206	-	-	0
19	LH206	Micronised	LH300	2.5
20	LH206	Micronised	LH300	5
21	LH206	Micronised	LH300	10
22	LH206	Micronised	LH300	20
23	LH206	Milled	LH230	2.5
24	LH206	Milled	LH230	5
25	LH206	Milled	LH230	10
26	LH206	Milled	LH230	20
27	LH206	Milled	LH210	2.5
28	LH206	Milled	LH210	5
29	LH206	Milled	LH210	10
30	LH206	Milled	LH210	20
31	SV010	-	-	0
32	SV010	Micronised	LH300	2.5
33	SV010	Micronised	LH300	5
34	SV010	Micronised	LH300	10
35	SV010	Micronised	LH300	20
36	SV010	Milled	LH210	2.5
37	SV010	Milled	LH210	5
38	SV010	Milled	LH210	10
39	SV010	Milled	LH210	20

Table II 10th, 50th and 90th percentiles (d10, d50 and d90 respectively) of particle size distributions coarse lactose carriers (LH100, LH206 and SV010) and the lactose fines (LH300, LH230, LH210 and Sorbolac 400) used in the study dispersed dry at 2 bar disperser pressure. The results are an average from five repeated measurements.

	d10 (µm)	**d50 (µm)**	**d90 (µm)**	**%<4.5**
LH100	44.3	103.37	159.62	1.29
LH206	49.78	93.05	142.21	2.44
SV010	49.61	108.78	166.78	1.55
LH300	0.84	2.41	7.76	77.13
LH230	1.31	8.05	21.97	35.68
LH210	1.64	14.3	39.45	23.84
Sorbolac 400	1.79	9.28	22.12	23.85

Table III Summary of particle size of the carrier pre-blends in terms of proportion of fines below 4.5, 15 and 30 µm and the 10th percentile of density distribution (d10) measured dispersed dry at 3 bar disperser pressure. The values shown are averages from five repeated measurements.

Carrier ID	Fines	<4.5 µm (%)	<15 µm (%)	<30 µm (%)	d10 (µm)
1	0%	1.29	3.02	6.24	44.3
2	2.5% Micronised	4.88	8.25	11.48	23.44
3	5% Micronised	9.34	13.94	17.03	5.22
4	10% Micronised	17.43	24.52	26.97	2.08
5	20% Micronised	23.04	40.24	42.75	1.73
6	2.5% Milled	2.76	6.70	10.95	26.41
7	5% Milled	4.32	10.15	15.13	14.7
8	10% Milled	7.23	16.78	23.23	7.33
9	20% Milled	12.47	28.93	38.15	3.26
10	2.5% Milled	1.98	5.14	9.56	31.53
11	5% Milled	2.62	6.78	12.27	23.63
12	10% Milled	4.08	10.44	17.89	14.25
13	20% Milled	6.02	15.91	26.79	8.72
14	2.5% Milled	2.37	6.23	10.05	29.77
15	5% Milled	3.32	9.20	13.81	17.01
16	10% Milled	5.88	15.60	21.72	8.68
17	20% Milled	10.20	27.62	36.7	4.39
18	0%	2.44	2.54	3.81	49.78
19	2.5% Micronised	6.13	8.11	9.27	34.3
20	5% Micronised	10.42	13.76	14.8	4.11
21	10% Micronised	18.16	24.42	25.24	1.95
22	20% Micronised	22.43	39.53	40.6	1.8
23	2.5% Milled	3.69	6.49	8.69	36.76
24	5% Milled	5.29	9.99	13.01	15.08
25	10% Milled	8.04	16.30	20.79	6.74
26	20% Milled	12.40	27.77	35.18	3.28
27	2.5% Milled	3.45	5.50	7.91	38.48
28	5% Milled	3.66	6.74	10.21	29.09
29	10% Milled	5.05	10.51	16.23	13.97
30	20% Milled	7.01	16.79	26.57	7.67
31	0%	1.55	3.03	5.19	49.61
32	2.5% Micronised	3.17	6.23	8.07	40.48
33	5% Micronised	6.51	11.75	13.57	9.18
34	10% Micronised	12.08	21.08	22.61	3.49
35	20% Micronised	22.47	38.05	39.33	1.74
36	2.5% Milled	2.01	4.41	7.46	40.97
37	5% Milled	2.57	6.03	10.16	29.42
38	10% Milled	3.63	9.29	15.53	16.54
39	20% Milled	6.53	16.38	26.27	8.13

Table IV Flow and fluidisation properties of the carrier pre-blends in terms of bulk and tapped densities, Hausner ratio, Basic flow energy (BFE_{Norm}), dynamic flow index (DFI), flow rate index (FRI), normalised fluidisation energy (FE_{Norm}) and specific energy (SE). The values shown are averages from three repeated measurements

Carrier ID	Fines	Bulk density (g/ml)	Tapped density (g/ml)	Hausner ratio	BFE_{Norm} (mJ/g)	DFI	FRI	FE_{Norm} (mJ/g)	SE (mJ/g)
1	0%	0.747	0.855	1.159	25.12	37.37	1.02	0.70	6.02
2	2.5% Micronised	0.727	0.854	1.224	22.06	27.90	1.10	0.84	5.84
3	5% Micronised	0.699	0.847	1.250	20.34	16.61	1.19	1.23	6.06
4	10% Micronised	0.667	0.860	1.380	15.68	10.87	1.52	1.44	6.25
5	20% Micronised	0.681	0.869	1.464	9.93	5.69	2.41	1.75	6.27
6	2.5% Milled	0.709	0.865	1.216	21.65	24.07	1.06	0.95	6.14
7	5% Milled	0.676	0.866	1.252	19.37	18.49	1.09	1.12	6.12
8	10% Milled	0.645	0.880	1.358	16.07	10.74	1.29	1.54	6.10
9	20% Milled	0.560	0.867	1.474	10.52	6.15	1.81	1.93	5.66
10	2.5% Milled	0.731	0.863	1.183	23.48	31.39	1.03	0.78	5.96
11	5% Milled	0.711	0.872	1.221	21.11	21.14	1.06	1.00	6.00
12	10% Milled	0.699	0.881	1.264	19.54	19.56	1.14	1.04	6.08
13	20% Milled	0.621	0.882	1.369	13.24	9.21	1.41	1.60	5.85
14	2.5% Milled	0.703	0.859	1.223	21.26	24.92	1.08	1.01	5.87
15	5% Milled	0.695	0.871	1.254	20.23	18.91	1.13	1.17	6.13
16	10% Milled	0.669	0.883	1.319	16.95	13.68	1.25	1.33	6.26
17	20% Milled	0.625	0.893	1.428	11.81	8.52	1.88	1.44	6.26
18	0%	0.744	0.861	1.135	22.67	30.23	1.08	0.82	5.58
19	2.5% Micronised	0.708	0.854	1.206	19.85	17.55	1.10	1.14	5.94
20	5% Micronised	0.668	0.857	1.284	17.60	11.74	1.16	1.53	6.09
21	10% Micronised	0.613	0.856	1.396	15.65	8.02	1.42	1.93	6.29
22	20% Micronised	0.604	0.875	1.449	9.96	4.96	2.27	1.88	6.21
23	2.5% Milled	0.725	0.881	1.214	21.00	23.78	1.08	0.93	6.20
24	5% Milled	0.692	0.874	1.264	19.71	15.90	1.09	1.41	6.59
25	10% Milled	0.663	0.877	1.324	15.75	10.55	1.27	1.56	6.29
26	20% Milled	0.575	0.883	1.537	11.48	6.06	1.66	1.89	5.96
27	2.5% Milled	0.733	0.869	1.186	21.47	28.66	1.05	0.81	5.68
28	5% Milled	0.720	0.873	1.212	19.68	21.50	1.09	1.00	5.70
29	10% Milled	0.683	0.879	1.288	17.36	15.27	1.15	1.22	5.99
30	20% Milled	0.635	0.885	1.395	13.34	9.70	1.39	1.49	6.01
31	0%	0.729	0.845	1.158	26.03	51.02	1.11	0.57	5.74
32	2.5% Micronised	0.729	0.858	1.177	23.60	41.61	1.10	0.57	5.72
33	5% Micronised	0.703	0.849	1.209	20.74	17.52	1.15	1.14	5.99
34	10% Micronised	0.636	0.855	1.344	9.55	9.55	1.32	1.91	6.17
35	20% Micronised	0.599	0.861	1.438	10.18	6.39	2.45	1.57	6.19
36	2.5% Milled	0.741	0.858	1.158	25.79	34.31	1.09	0.80	5.80
37	5% Milled	0.725	0.865	1.193	22.83	31.65	1.10	0.78	5.76
38	10% Milled	0.687	0.862	1.255	18.95	24.34	1.15	1.03	5.90
39	20% Milled	0.645	0.887	1.375	15.35	10.63	1.43	1.52	6.21

Table V Summary of *in vitro* performance of the formulations prepared with the lactose pre-blends as the carrier in terms of fine particle fraction of emitted dose (FPF_{ED}), mean mass aerodynamic diameter (MMAD) and the proportion of total recovered budesonide that was deposited in the pre-separator (PS of RD). The results shown are averages from three repeated *in vitro* assessments.

Carrier ID	Fines	FPF of ED (%)	MMAD (μm)	PS of RD (%)
1	0%	24.10	2.58	38.23
2	2.5% Micronised	26.56	2.94	31.00
3	5% Micronised	35.78	3.04	21.17
4	10% Micronised	46.94	3.09	13.37
5	20% Micronised	39.74	3.36	12.74
6	2.5% Milled	23.85	2.78	35.15
7	5% Milled	25.32	3.00	31.68
8	10% Milled	28.21	3.26	21.63
9	20% Milled	35.95	3.25	15.42
10	2.5% Milled	23.13	2.75	37.09
11	5% Milled	24.14	2.85	33.94
12	10% Milled	27.38	3.00	25.87
13	20% Milled	26.63	3.14	23.97
14	2.5% Milled	21.03	2.86	42.90
15	5% Milled	22.08	2.92	37.80
16	10% Milled	27.19	3.04	28.27
17	20% Milled	26.90	3.51	20.47
18	0%	24.56	2.62	39.31
19	2.5% Micronised	32.49	2.81	27.04
20	5% Micronised	36.09	2.92	21.73
21	10% Micronised	44.71	3.19	13.63
22	20% Micronised	36.73	3.48	14.53
23	2.5% Milled	25.50	2.78	32.30
24	5% Milled	26.75	2.89	28.46
25	10% Milled	28.69	3.15	23.31
26	20% Milled	32.89	3.34	18.56
27	2.5% Milled	23.28	2.70	38.94
28	5% Milled	25.11	2.79	34.34
29	10% Milled	24.33	2.88	30.23
30	20% Milled	30.41	3.01	22.93
31	0%	20.82	2.65	44.25
32	2.5% Micronised	23.28	2.96	34.95
33	5% Micronised	30.63	3.04	27.09
34	10% Micronised	39.65	3.12	17.12
35	20% Micronised	35.15	3.40	13.84
36	2.5% Milled	22.26	2.77	41.25
37	5% Milled	23.05	2.91	40.17
38	10% Milled	24.42	3.02	36.12
39	20% Milled	25.52	3.01	23.49

Table VI Coefficient of correlation (*r*) for linear relationships between the different DPI performance measures and the properties of the lactose pre-blends used as the carriers in the formulations. The correlations are based on the average values reported in Tables IV, V and VI.

	Correlation coefficient (*r*)		
	FPF_{ED}[1]	**MMAD[2]**	**PS of RD[3]**
<4.5 µm	0.861	0.793	-0.882
<15 µm	0.740	0.907	-0.885
<30 µm	0.638	0.924	-0.862
d10	-0.687	-0.839	0.867
Bulk density	-0.589	-0.839	0.805
Tapped density	-0.147	0.368	-0.226
Hausner ratio	0.649	0.889	-0.866
BFE_{Norm}	-0.664	-0.864	0.872
DFI	-0.673	-0.784	0.870
FRI	0.578	0.825	-0.741
FE_{Norm}	0.748	0.800	-0.891
SE	0.413	0.431	-0.533

[1] Fine particle fraction of emitted dose (FPF_{ED})

[2] Mean mass aerodynamic diameter (MMAD)

[3] Proportion of budesonide recovered from the pre-separator (PS of RD)

Table VII The connection weights for the different input parameters in the neural networks describing DPI performance. The networks were based on the average values reported in Tables IV, V and VI.

	Connection weights (%)		
	FPF_{ED}[1]	**MMAD[2]**	**PS of RD[3]**
%<4.5	56.94	2.50	45.76
%<15	0.09	75.56	1.05
%<30	1.24	0.45	5.27
d10	3.64	4.82	19.17
BFE_{Norm}	0.57	0.08	9.05
Bulk density	6.78	1.99	7.78
Tapped density	3.75	1.56	3.45
Hausner ratio	4.91	4.45	0.43
DFI	7.90	0.37	4.21
FE_{Norm}	0.13	7.15	2.88
FRI	13.65	0.18	0.03
SE	0.41	0.88	0.92

[1] Fine particle fraction of emitted dose (FPF_{ED})

[2] Mean mass aerodynamic diameter (MMAD)

[3] Proportion of budesonide recovered from the pre-separator (PS of RD)

Legend to figures

Figure 1. Particle size distribution of budesonide measured dispersed wet. The data represented is an average from five repeated measurements.

Figure 2. Cohesive-adhesive balance (CAB) plot for the batch of budesonide. The dotted line represents $F_{coh}=F_{adh}$ and corresponds to CAB value of 1.

Figure 3. Particle size distributions of lactoses measured dry dispersed at 2 bar disperser pressure. Black lines represent the coarse carriers (LH100, LH206 and SV010), light grey micronised lactose (LH300) and dark grey milled lactose grades (LH230, LH210 and Sorbolac 400). The data represents an average of five repeated measurements.

Figure 4. Coefficients of correlation (*r*) for linear correlations between different parameters describing the properties of the lactose carriers and A) fine particle fraction of emitted dose B) mean mass aerodynamic diameter and C) pre-separator deposition of budesonide.

Figure 5. The relative importance of the different input parameters (connection weights) in the neural network modelling the relationship between the parameters describing the properties of the lactose carrier and A) fine particle fraction of emitted dose B) mean mass aerodynamic diameter and C) pre-separator deposition of budesonide

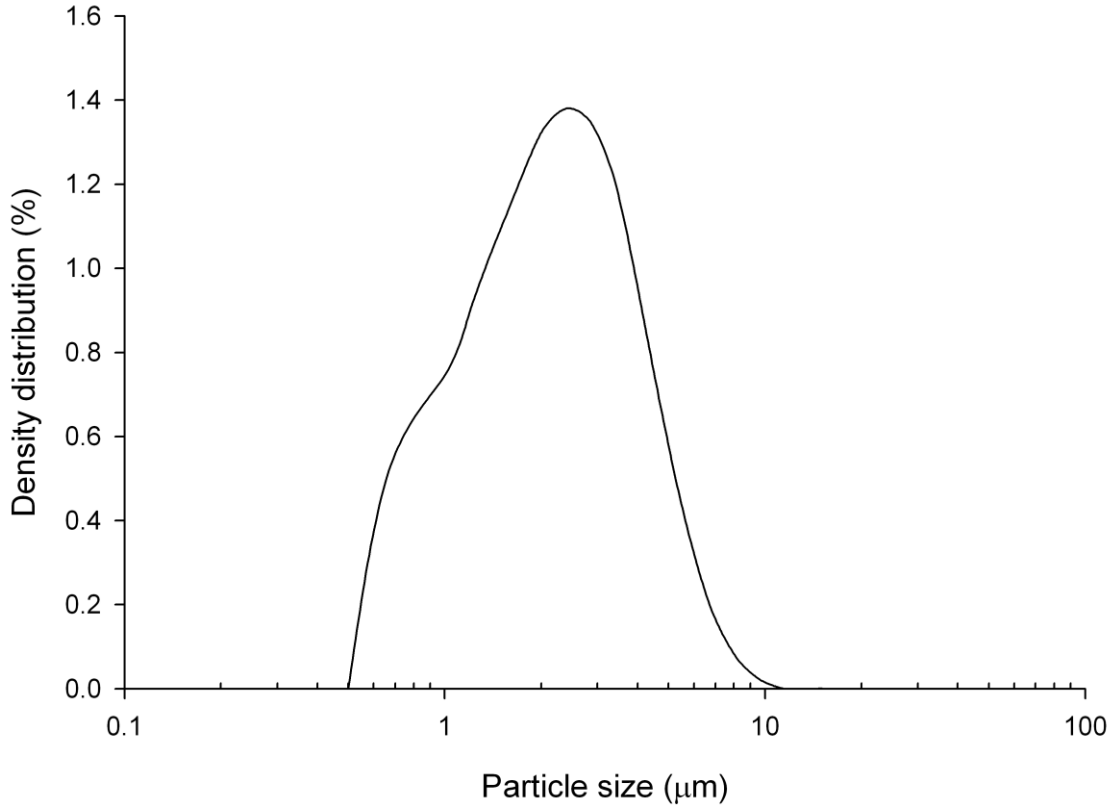
1.6
1.4
1.2
1.0
0.8
0.6
0.4
0.2
0.0
Density distribution (%)
0.1
1
10
100
Particle size (μm)

Figure 1.

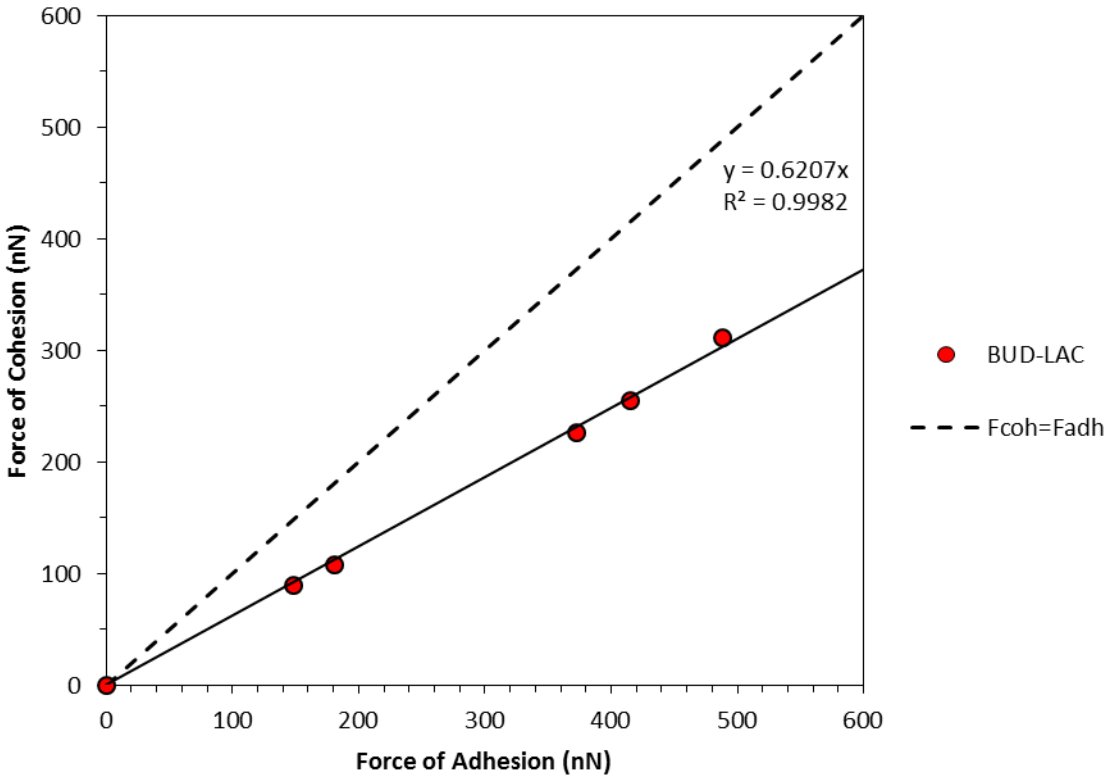
600
500
400
300
200
100
0
0
100
200
300
400
500
600
Force of Cohesion (nN)
Force of Adhesion (nN)
y = 0.6207x
R² = 0.9982
BUD-LAC
Fcoh=Fadh

Figure 2.

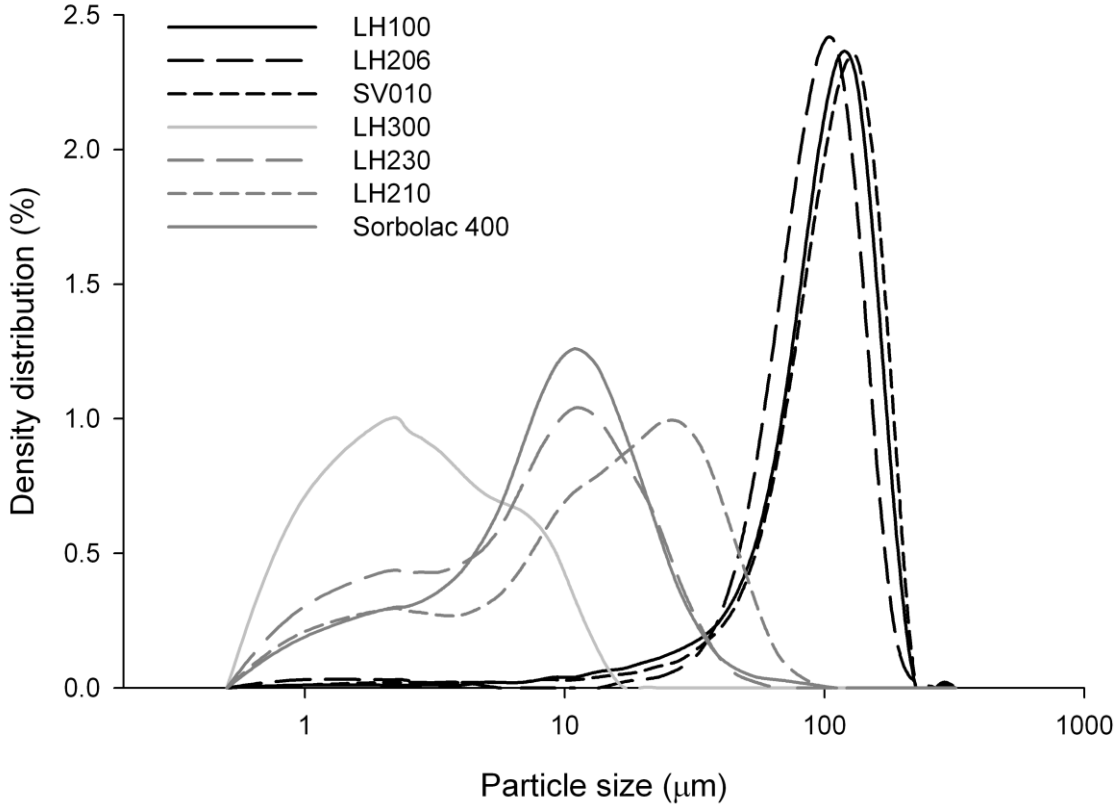
LH100
LH206
SV010
LH300
LH230
LH210
Sorbolac 400
Density distribution (%)
2.5
2.0
1.5
1.0
0.5
0.0
1
10
100
1000
Particle size (μm)

Figure 3.

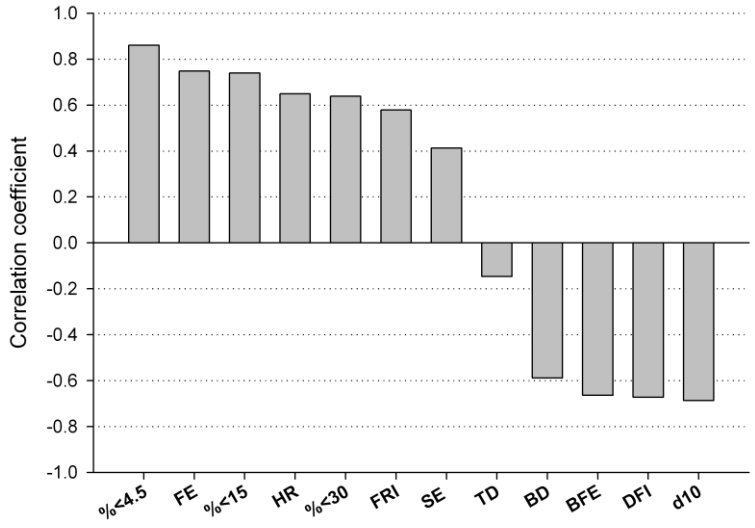
Correlation coefficient
1.0
0.8
0.6
0.4
0.2
0.0
-0.2
-0.4
-0.6
-0.8
-1.0
%<4.5
FE
%<15
HR
%<30
FRI
SE
TD
BD
BFE
DFI
d10

A

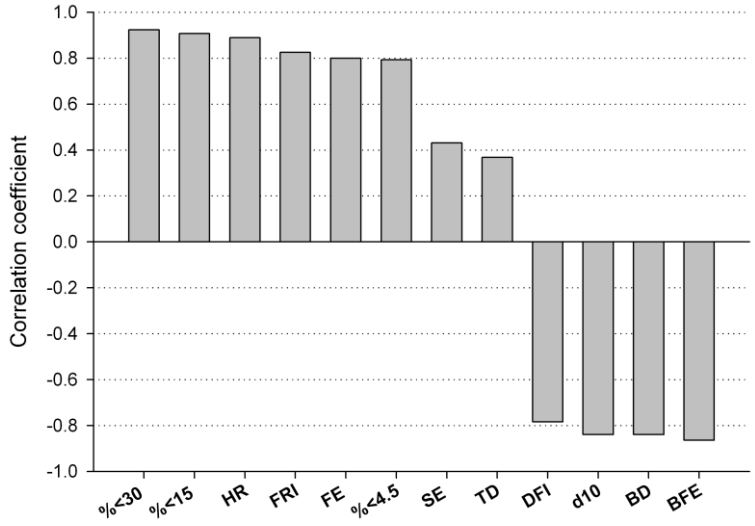
Correlation coefficient
1.0
0.8
0.6
0.4
0.2
0.0
-0.2
-0.4
-0.6
-0.8
-1.0
%<30
%<15
HR
FRI
FE
%<4.5
SE
TD
DFI
d10
BD
BFE

B

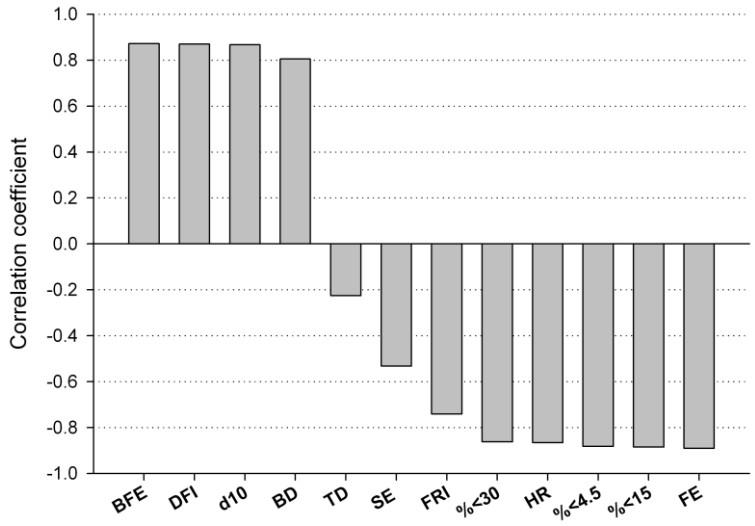
Correlation coefficient
1.0
0.8
0.6
0.4
0.2
0.0
-0.2
-0.4
-0.6
-0.8
-1.0
BFE
DFI
d10
BD
TD
SE
FRI
%<30
HR
%<4.5
%<15
FE

C

Figure 4.

A

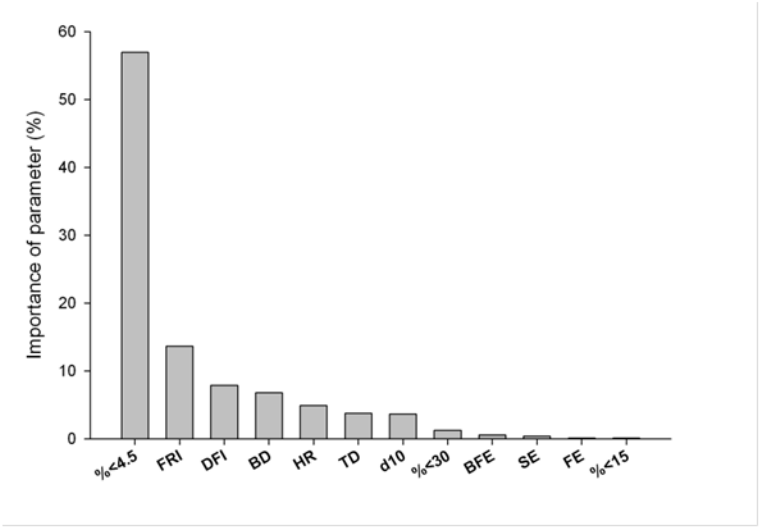
Importance of parameter (%)
60
50
40
30
20
10
0
%<4.5
FRI
DFI
BD
HR
TD
d10
%<30
BFE
SE
FE
%<15

B

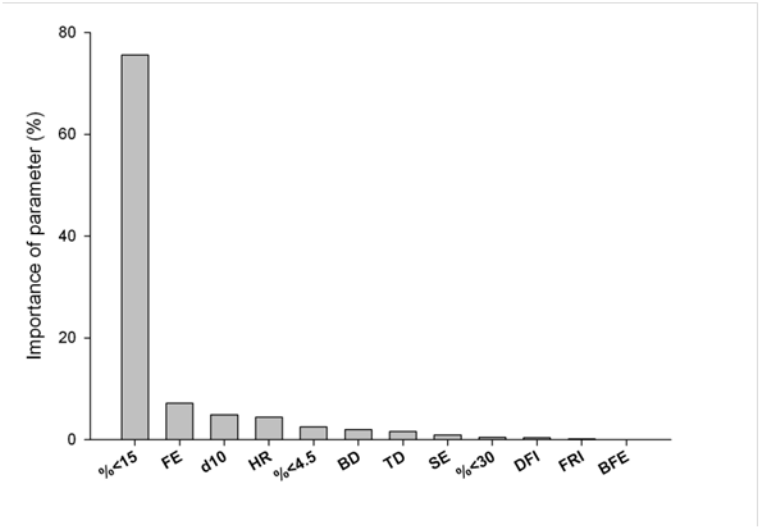
Importance of parameter (%)
80
60
40
20
0
%<15
FE
d10
HR
%<4.5
BD
TD
SE
%<30
DFI
FRI
BFE

C

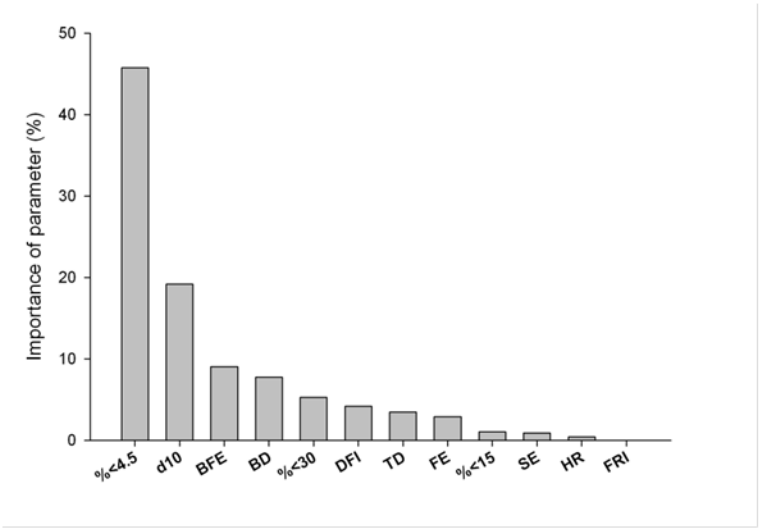
Importance of parameter (%)
50
40
30
20
10
0
%<4.5
d10
BFE
BD
%<30
DFI
TD
FE
%<15
SE
HR
FRI

Figure 5.